APPLIED AND ENVIRONMENTAL MICROBIOLOGY, Dec. 2004, p. 6968–6976 Vol. 70, No. 12
0099-2240/04/$08.00+0 DOI: 10.1128/AEM.70.12.6968–6976.2004

Use of *Pseudomonas putida* EstA as an Anchoring Motif for Display of a Periplasmic Enzyme on the Surface of *Escherichia coli*

Taek Ho Yang,[1] Jae Gu Pan,[2] Yeon Soo Seo,[1] and Joon Shick Rhee[1]*

Department of Biological Sciences, Korea Advanced Institute of Science and Technology,[1] and National Research Laboratory for Microbial Display, GenoFocus Inc., Daeduk BioCommunity,[2] Daejeon, Republic of Korea

Received 20 May 2004/Accepted 17 July 2004

The functional expression of proteins on the surface of bacteria has proven important for numerous biotechnological applications. In this report, we investigated the N-terminal fusion display of the periplasmic enzyme β-lactamase (Bla) on the surface of *Escherichia coli* by using the translocator domain of the *Pseudomonas putida* outer membrane esterase (EstA), which is a member of the lipolytic autotransporter enzymes. To find out the transport function of a C-terminal domain of EstA, we generated a set of Bla-EstA fusion proteins containing N-terminally truncated derivatives of the EstA C-terminal domain. The surface exposure of the Bla moiety was verified by whole-cell immunoblots, protease accessibility, and fluorescence-activated cell sorting. The investigation of growth kinetics and host cell viability showed that the presence of the EstA translocator domain in the outer membrane neither inhibits cell growth nor affects cell viability. Furthermore, the surface-exposed Bla moiety was shown to be enzymatically active. These results demonstrate for the first time that the translocator domain of a lipolytic autotransporter enzyme is an effective anchoring motif for the functional display of heterologous passenger protein on the surface of *E. coli*. This investigation also provides a possible topological model of the EstA translocator domain, which might serve as a basis for the construction of fusion proteins containing heterologous passenger domains.

In recent years, the display of heterologous proteins on the surface of microorganisms has been extensively investigated due to a wide range of biotechnological and industrial applications such as live vaccine development, high-throughput screening, whole-cell biocatalysts, and bioadsorbents (3, 8, 30). A variety of native surface proteins and their partial fragments of bacteria have been exploited as a surface anchoring motif. In gram-negative bacteria, outer membrane proteins (1, 12, 50), lipoproteins (7, 13, 21), autotransporter proteins (23, 29, 46, 48), some secretory proteins (27), subunits of cellular appendix proteins (25, 33), and S-layer proteins (4) have been exploited as an anchoring motif, while staphylococcal protein A (43) and S-layer homology domain (37) have been used in gram-positive bacteria. Owing to the relative simplicity of its transporting mechanism, the autotransporter-mediated surface display (autodisplay) system has been employed successfully for the display of receptor or ligand for purification or binding assays (48), expression of peptide libraries for epitope mapping or antibody specificity tests (26), functional domain analyses of heterologous proteins (23), bioconversion by expressing enzymatic activity on the bacterial surface (18, 29), and exposure of antigenic determinants for vaccine development (28). As the autodisplay system uses the N-terminal fusion approach, it might be suitable for display of foreign proteins whose N-terminal region is essential for their biological activity or foreign proteins which have a native N-terminal signal sequence for translocating the inner membrane.

Autotransporters are virulence-related proteins of gram-negative bacteria. Members of the autotransporter family are featured by three domains: the signal sequence, the passenger domain, and the translocator domain (10). An N-terminal signal sequence directs the polypeptide through the Sec apparatus and into the periplasm. The translocator domain consists of a short linking region having an α-helical secondary structure and a β-domain that integrates into the outer membrane and forms a central hydrophilic pore, allowing the internal passenger domain to be presented on the bacterial surface (16). Generally, the β-domain of autotransporters is about 250 to 300 amino acid residues in length and exhibits 14 antiparallel amphipathic β-strands that make up the β-barrel structure in the outer membrane (10). The passenger domain confers the diverse effector functions to the autotransporters. This passenger domain may stay attached to the cell surface, anchored by the translocator domain. However, many passengers contain a protease subdomain which may mediate release by autocatalytic processing (16). Alternatively, other outer membrane proteins such as membrane-bound proteases may be involved in processing.

In the course of finding the genes encoding lipolytic enzymes in *Pseudomonas putida* 3SK, the well-known solvent-tolerant strain, we identified an esterase gene (*estA*) whose deduced amino acid sequence was identical with that of the outer membrane esterase from *P. aeruginosa* PAO1 (gene identification number 2218156) (Fig. 1A). EstA is a member of the lipolytic autotransporter enzymes (15, 49). This family of enzymes is characterized by an active site Ser residue that is located very close to the N terminus within the sequence GDSL and the sequence surrounding the residues involved in the catalytic triad (D, S, and H residues) that is different from the analogous residues in the trypsin-like serine proteases (15, 47). However, neither the physiological function of these lipolytic

* Corresponding author. Mailing address: Department of Biological Sciences, Korea Advanced Institute of Science and Technology, 373-1, Guseong-dong, Yuseong-gu, Daejeon 305-701, Republic of Korea. Phone: 82-42-869-2613. Fax: 82-42-869-2610. E-mail: jsrhee1@webmail.kaist.ac.kr.

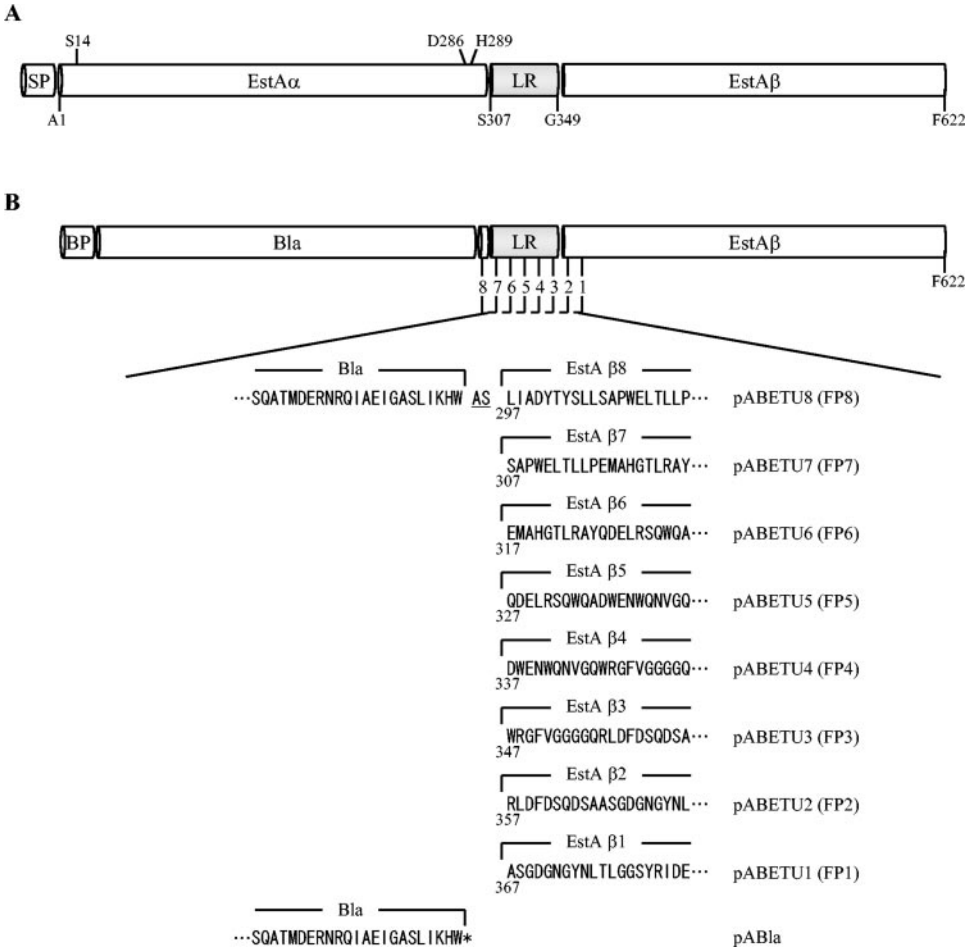

FIG. 1. (A) Schematic representation of the structure of the EstA preprotein. The EstA preprotein is predicted to be composed of a 24-amino-acid signal sequence (SP), the α-domain (EstAα) including the catalytic triad, the linking region (LR), and the β-domain (EstAβ). The amino acids indicated in the EstAα region show a putative catalytic triad (serine 14, aspartate 286, and histidine 289). The predicted linking region (S307 to G349) is assumed to contain an α-helical structure. (B) Schematic representation of the construction of the Bla-EstA fusion proteins. The fusion protein is composed of the Bla signal sequence (BP) and the mature portion of Bla, fused to successively truncated C-terminal portions (numbered 1 to 8) of the EstA. Additional amino acids between Bla and the EstA C-terminal domain which were derived from a restriction enzyme site (NheI) for linking *bla* and each *estA* C-terminal region are underlined. Recombinant plasmids pABETU1 to pABETU8 encode the fusion proteins FP1 to FP8, respectively. As a control construct, pABla encodes wild-type Bla in the periplasm.

autotransporter enzymes nor their potential for biotechnological applications has been clearly characterized compared with other autotransporter proteins such as immunoglobulin A1 (IgA1) (24), antigen 43 (23), and AIDA-I (41). The translocation of passenger proteins may be related to their size and folding and may be different for each autotransporter β-domain. Therefore, it is difficult to predict whether a heterologous protein may be secreted by these systems, and this has to be determined case by case. In present study, we investigated the transport function of the EstA C-terminal domain by using analysis of the secondary structure prediction and translational fusions of the periplasmic enzyme β-lactamase (Bla) with N-terminally truncated EstA C-terminal domains. The expression of the various fusion proteins was monitored, and the surface exposure of the Bla moiety was examined. Based on these results, we predict the sufficient structure necessary for surface expression of the passenger domain and thus propose a possible topological model of the EstA translocator domain in the outer membrane. Finally, we show that the EstA translocator domain-mediated surface display system functionally exports Bla moieties on the surface of *Escherichia coli* cells in a stable manner without detrimental effects on host cell viability and outer membrane integrity.

MATERIALS AND METHODS

Bacterial strains and plasmids. The bacterial strains and plasmids used in this study are listed in Table 1. For all purposes, *E. coli* strains were grown at 37 or 25°C on Luria-Bertani (LB) agar or in LB broth supplemented with appropriate antibiotics unless otherwise stated, and *P. putida* 3SK was grown at 30°C in LB broth. The antibiotics used were ampicillin at 100 μg/ml, chloramphenicol at 30 μg/ml, and kanamycin at 25 μg/ml.

Recombinant DNA manipulations. For the construction of a genomic library of *P. putida* 3SK, genomic DNA was partially digested with Sau3AI, and fragments of about 8 to 15 kb in length were obtained from the agarose gel by using a QIAEX II gel extraction kit (QIAGEN, Valencia, Calif.). The pooled genomic DNA fragments were ligated into pUC19 that had been digested with BamHI and dephosphorylated. The ligation mixture was used to transform *E. coli* XL1-Blue, and the individual clones were plated onto esterase indicator plates containing tributyrin (49) to detect the formation of clear halos. From a library consisting of 12,000 transformants, several halo-forming clones were detected.

TABLE 1. Bacterial strains and plasmids used in this study

Strain or plasmid	Relevant characteristics	Reference or source
Strains		
P. putida 3SK	Outer membrane esterase (EstA) producer	32
E. coli BL21 (DE3)	F^- *ompT hsdSB* (r_B^- m_B^-) *gal dcm* (*lcIts857 ind1 Sam7 nin5 lacUV5-T7 gene1*)	Novagen
E. coli JM109	*recA1 endA1 gyrA96 thi-1 hsdR17 supE44 relA1* Δ(*lac-proAB*) [F′ *traD36 proAB*$^+$ *lacI*^{q} ZΔ15]	Stratagene
E. coli JK321	UT5600 *zih*::Tn*10 dsbA*::*kan*	19
E. coli UT5600	*azi-6 fhuA23 lacY1 leu-6 mtl-1 proC14 purE42 rpsL109 thi-I trpE38 tsx-67* D(*ompT-fepC*)	New England Biolabs
E. coli XL1-Blue	*recA1 endA1 gyrA96 thi-1 hsdR17 supE44* [F′ *proAB lacI*^{q}ZΔ15 Tn*10* (Tet^r)]	Stratagene
Plasmids		
pACYC184	*orip*P15A Cm^r Tet^r	42
pUC19	ColE1 Ap^r *lacI* ϕ80d*lacZ*	Takara
pESTE	EstA, derivative of pUC19	This study
pABla	Periplasmic Bla, derivative of pACYC184	This study
pABETU1	57.3-kDa Bla-EstA fusion proteins, derivative of pACYC184	This study
pABETU2	58.6-kDa Bla-EstA fusion proteins, derivative of pACYC184	This study
pABETU3	59.6-kDa Bla-EstA fusion proteins, derivative of pACYC184	This study
pABETU4	60.9-kDa Bla-EstA fusion proteins, derivative of pACYC184	This study
pABETU5	62.1-kDa Bla-EstA fusion proteins, derivative of pACYC184	This study
pABETU6	63.3-kDa Bla-EstA fusion proteins, derivative of pACYC184	This study
pABETU7	64.4-kDa Bla-EstA fusion proteins, derivative of pACYC184	This study
pABETU8	65.5-kDa Bla-EstA fusion proteins, derivative of pACYC184	This study

After an assay for lipase and esterase activity as previously described (49), one clone harboring a 9.0-kb fragment was selected for further investigation. The recombinant plasmid isolated from this clone was designated pESTE.

To construct the Bla-EstA fusions, the *bla* gene was amplified by PCR from plasmid pBR322 (5). The PCR fragment was digested with ClaI and NheI, fused to various 3′ portions of the gene encoding EstA which differed in length, and inserted into the Tet^r gene of plasmid vector pACYC184. The *estA* 3′ regions used to generate constructs employed in this study were amplified from a plasmid preparation of pESTE by PCR. The resulting plasmids contained a genetic fusion of the *bla* gene with the various EstA C-terminal domains (Fig. 1B); the expression of the corresponding fusion protein is driven by the promoter of the *bla* gene. As a control, the plasmid (pABla) expressing wild-type Bla in the periplasm was also constructed (Fig. 1B).

The enzymes and related reagents for DNA manipulation used in this study were obtained from New England Biolabs Inc. (Beverley, Mass.), TaKaRa Shuzo Co. (Shiga, Japan), and Sigma Chemical Co. (St. Louis, Mo.). Preparation of plasmids and DNA fragments was performed with QIAGEN kits (QIAGEN). DNA sequencing was carried out by using AmpliTaq DNA polymerase (Perkin-Elmer, Foster City, Calif.) on an ABI PRISM 377 DNA sequencer.

Immunoblot analysis. The expression of wild-type Bla and fusion proteins was analyzed by the whole-cell lysate of *E. coli* using Western blots. After sodium dodecyl sulfate-polyacrylamide gel electrophoresis, the samples were electroblotted onto polyvinylidene difluoride membranes and probed with Bla-specific monoclonal antibody (QED Bioscience Inc., San Diego, Calif.) diluted 1:2,000 in Tris-buffered saline (TBS) (150 mM NaCl, 50 mM Tris-HCl [pH 7.4]) containing 1% gelatin and 0.05% Tween 20. Immunoblots were rinsed three times with TBS containing 0.05% Tween 20 prior to the addition of secondary antibody. Antigen-antibody complexes were visualized by reaction to horseradish peroxidase-linked goat anti-mouse IgG secondary antibody (Sigma) diluted 1:5,000 in TBS. A color reaction of horseradish peroxidase was done according to the manufacturer's instructions (Bio-Rad, Hercules, Calif.).

For whole-cell immunoblots, bacteria grown overnight were harvested from LB agar plates, washed three times with phosphate-buffered saline (PBS) (pH 7.4), and resuspended to an optical density at 600 nm (OD_{600}) of 10.0. Aliquots of 2 μl were applied to a nitrocellulose membrane (Bio-Rad) and allowed to dry completely. Subsequently, the immunodetection was performed as described above.

Protease accessibility. *E. coli* cells were collected from the LB agar plates and washed three times with PBS. Subsequently, the bacterial suspension was adjusted to an OD_{600} of 10.0. Two microliters of trypsin stock solution was added to 200 μl of suspension to yield a final concentration of 50 μg/ml. Suspensions were incubated for 20 min at 37°C, and digestion was stopped by washing the cells three times with PBS. Cells were collected by brief centrifugation and subjected to Western blotting and whole-cell immunoblotting. For the whole-cell immunoblot analysis, 2 μl of bacterial cell suspensions was directly applied to a nitrocellulose membrane (Bio-Rad) and allowed to dry completely before proceeding to next procedure.

Flow cytometry analysis. For immunofluorescence staining, *E. coli* cells were collected from the LB agar plates or harvested from LB broth culture and washed three times with PBS. Subsequently, the bacterial suspension was adjusted to an OD_{600} of 0.5 and resuspended in 1 ml of PBS solution containing 1% bovine serum albumin and Bla-specific monoclonal antibody (1:1,000). Incubation on ice for 1 h was sufficient to allow the primary antibody to bind to its antigen. After being washed three times with PBS, the cells were incubated with the fluorescein isothiocyanate-labeled anti-mouse IgG goat antibody (Sigma) diluted 1:100 in PBS for 1 h on ice, washed five times with PBS, and resuspended in 500 μl of PBS. These cells were examined with a FACScan flow cytometer (Becton Dickinson, Oxnard, Calif.). Samples were illuminated with an argon laser (488 nm), and fluorescence emission was detected at 510 to 530 nm (FL1 channel). For each sample, 50,000 events were counted at a rate between 500 and 1,000 events/s.

Cell viability assay. The viability of recombinant *E. coli* cells was estimated by using membrane potential probe bis-(1,3-dibutylbarbituric acid)trimethine oxonol [$DiBAC_4(3)$; Molecular Probes Inc., Eugene, Oreg.] as previously described (17). Bacterial culture samples were removed from the flasks and resuspended in PBS (approximately 10^6 to 10^7 cells/ml) containing 1 μM $DiBAC_4(3)$. Cells were allowed to stain at room temperature for 10 min before flow cytometry analysis.

Whole-cell Bla activity assay. Whole-cell Bla activity was determined by essentially the same method as that described previously (29). *E. coli* cells expressing surface-displayed Bla were collected from LB agar plates or harvested from LB broth culture and washed three times with PBS. The washed suspension was adjusted to an OD_{575} of 10.0. Subsequently, 200 μl of this suspension was incubated at room temperature with 50 μl of a penicillin G solution (10 mg/ml). After 10 min, PBS was added to a final volume of 1 ml. After a brief centrifugation at 13,000 × *g* to remove the cells, the penicillin G content of the supernatant was analyzed by spectrophotometry at 240 nm. As a control, the same assay was performed without incubation for 10 min to obtain normalized ΔOD values for each experiment.

Nucleotide sequence accession number. The sequence of the *estA* gene has been submitted to GenBank under accession number AY676875.

RESULTS

Cloning and sequence analysis of EstA from *P. putida* 3SK. Esterase gene (*estA*) was cloned and sequenced from the genomic library of *P. putida* 3SK on esterase indicator plates containing tributyrin. Interestingly, a protein-protein BLAST (2) analysis of *estA* revealed that the deduced amino acid sequence was identical with that of the outer membrane esterase from *P. aeruginosa* PAO1 (49) and that other homologues

TABLE 2. Proteins identified as showing high percent sequence similarity with EstA of *P. putida* 3SK

Protein	Characteristic	Organism	Size (aa[c])	Identity (%)	Consensus motif	GI no.[b]
EstA[a]	Outer membrane esterase	*P. aeruginosa* PAO1	646	100	GDSLS	2218156
PalA	Autotransporting lipolytic enzyme	*Pseudomonas* sp. strain HSM0414	636	65.8	GDSLS	15810051
Pflu4062	Phospholipase/lecithinase/hemolysin	*P. fluorescens* PfO-1	636	65.0	GDSLS	23061978
PsEst1	Esterase	*Pseudomonas* sp. strain B11-1	637	64.1	GDSLN	23978942
PSPTO0569	Autotransporting lipase, GDSL family	*P. syringae* pv. Tomato strain DC3000	640	62.1	GDSLA	28851032
Psyr0058	Phospholipase/lecithinase/hemolysin	*P. syringae* pv. Syringae B728a	658	60.1	GDSLA	23468450
PP0418	Lipase, GDSL family	*P. putida* KT2440	629	60.8	GDSLA	26987159
Ytrp	Hypothetical 62.7-kDa protein in *trpE-trpG* intergenic region	*P. putida* PPG1 C1S	592	55.4	GDSLS	732298

[a] The deduced amino acid sequence is found to be identical with that of EstA of *P. putida* 3SK.
[b] GI, gene identification.
[c] aa, amino acids.

which showed a high percent sequence similarity were found mainly in *Pseudomonas* strains (Table 2). On the basis of conserved domain analysis (34), all of these proteins belong to a family of lipolytic autotransporter enzymes (15).

The esterase encoded by *estA* is synthesized as a precursor of 646 amino acids with a predicted 24-amino-acid signal sequence for transport across the inner membrane. According to an investigation done by Wilhelm et al. (49), EstA may remain tightly attached to the outer membrane in both *P. aeruginosa* and *E. coli*. Furthermore, they proposed tentative topological model of the C-terminal β-domain contrary to the typical structure of an autotransporter. In this model, the C-terminal domain (Y374 to F622) of EstA is predicted to consist of 11 amphipathic β-strands, and the β-barrel may consist of as few as 10 β-strands with the first one reaching through the interior of the barrel, thereby exposing the passenger domain to the cell surface. Alternatively, the barrel formed may not be closed, creating instability of the overall β-domain structure. However, an analysis of the secondary structure of the EstA C-terminal 316 amino acids (S307 to F622) using the 3D-PSSM program (22) identified an α-helical structure and an additional hypothetical β-strand together with 11 amphipathic β-strands which were predicted by Wilhelm et al. (49). Thus, we supposed tentatively that the stretch of amino acids from S307 to G373 of EstA might play a role in β-barrel formation or in translocation of the passenger domain (Fig. 1A).

Construction of recombinant gene fusions. To investigate both the possibility of displaying heterologous passenger protein with the EstA translocator domain and the sufficient structure necessary for surface exposure of the N-terminal passenger protein, we constructed a series of fusion proteins which contain Bla and N-terminally truncated EstA C-terminal domains (Fig. 1B). The normally periplasmic enzyme Bla has been frequently employed as a reporter protein for the investigation of surface expression function of anchoring motifs in *E. coli* (12, 27, 29). Based on a secondary structure prediction using the 3D-PSSM program, the fusion points were designed to give rise to five different lengths of the predicted linking region, resulting in EstA β3 to EstA β7. Two additional N-terminal deletions (EstA β1 and EstA β2) were set within the predicted β-domain of EstA, and one more deletion (EstA β8) was positioned 10 amino acids in front of the predicted linking region. The shortest deletion (EstA β1) started with A367, which was thought to contain only the 11 amphipathic β-strands. The resulting plasmids encoded the Bla-EstA fusion proteins, FP1 to FP8, and were designated pABETU1 to pABETU8, respectively (Fig. 1B). As a control, the pABla expressing wild-type Bla in the periplasm was also constructed. All fusion proteins and wild-type Bla were expressed under the control of the native promoter of the *bla* gene, and the Bla signal sequence was used to ensure the transport of the fusion proteins across the cytoplasmic membrane.

Expression of *bla-estA* gene fusions. This set of eight different Bla-EstA fusion proteins and periplasmic Bla were expressed by using *E. coli* JK321 (*dsbA ompT*) as a host strain. JK321 is known as a suitable strain for stable display of a cysteine-containing passenger on the surface of *E. coli* cells via the autotransporter pathway (19, 29, 36). As revealed by the Western blot analysis of total lysates of *E. coli* JK321 transformants with anti-Bla antibody, all fusion proteins and periplasmic Bla can be detected with expected size (Fig. 2A). However, the expression levels of fusion proteins varied significantly despite the identical background used. The Bla-EstA fusion protein FP8 was expressed at the highest level, followed by FP7 and FP6, comprising smaller portions of EstA C-terminal domain, while very poor expression was observed for FP1 through FP5. Furthermore, to investigate the transport function of the EstA translocator domain, we initially tested the presence of the Bla moiety on the surface of *E. coli* cells by using whole-cell immunoblot analysis. Physiologically intact recombinant *E. coli* cells were applied directly to nitrocellulose membrane, and the immunodetection was subsequently performed. As shown in Fig. 2B, *E. coli* cells expressing the Bla-EstA fusion proteins FP6 through FP8 exhibited the specific antigen-antibody immunoreaction, while cells expressing FP1 through FP5 and periplasmic Bla did not. The color intensity of the whole-cell immunoblot, which indicates the amount of Bla molecules, was found to correlate with the expression level of the fusion proteins and depend on the length of EstA C-terminal domain, as shown by Western blots. This result demonstrates that the fusion proteins FP6 through FP8 appear to be localized in the outer membrane of *E. coli* exposing the Bla moiety.

Both the outer membrane protease OmpT and the periplasmic oxidoreductase DsbA have been shown to influence the surface expression of passenger proteins (19, 35). To examine the influence of *dsbA* and *ompT* mutations on the surface expression of Bla, the fusion proteins were expressed in various *E. coli* strains, JK321 (*dsbA ompT*), UT5600 (*ompT*), BL21(DE3) (*ompT*), JM109, and XL1-Blue (Fig. 2C). Whole-cell immunoblot analysis revealed that the surface expression was most

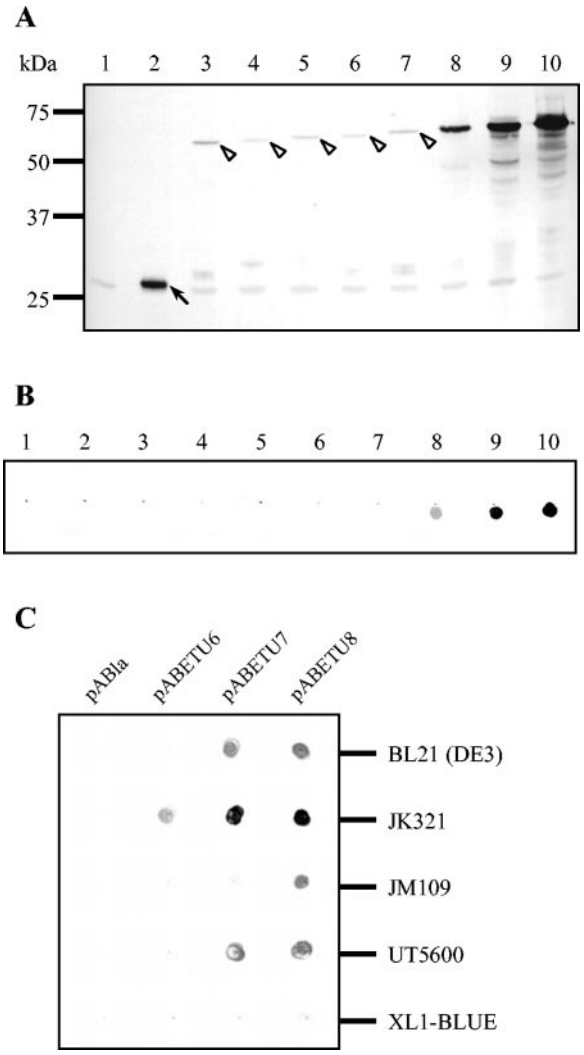

FIG. 2. (A) Expression of fusion proteins in *E. coli* as assessed by Western blots. Equal amounts of whole-cell lysates of recombinant *E. coli* JK321 cells corresponding 10 μl of a suspension with an OD_{600} of 10.0 were separated by sodium dodecyl sulfate-polyacrylamide gel electrophoresis and subsequent Western blot analysis with anti-Bla antibody. Lane 1, pACYC184 (vector); lane 2, pABla; lane 3, pABETU1; lane 4, pABETU2; lane 5, pABETU3; lane 6, pABETU4; lane 7, pABETU5; lane 8, pABETU6; lane 9, pABETU7; lane 10, pABETU8. The poorly expressed fusion proteins are indicated by the open arrowheads (lanes 3 to 7), and periplasmic expressed Bla-derived bands are indicated with an arrow (lane 2). (B) Surface exposure of fusion proteins assessed by whole-cell immunoblots. Equal amounts of recombinant *E. coli* JK321 cell suspensions were applied directly to nitrocellulose membrane and subsequently subjected to immunodetection analysis. Each lane is the same as those described for panel A. (C) Surface exposure of fusion proteins in various *E. coli* strains assessed by whole-cell immunoblots. Equal amounts of recombinant *E. coli* cell suspensions were applied directly to nitrocellulose membrane and subsequently subjected to immunodetection analysis.

efficient in the *ompT dsbA* strain JK321, followed by other *ompT* strains, BL21 (DE3) and UT5600. We also found that the translocation of the Bla moiety was more efficient in the *dsbA* strain JK321 than in its otherwise isogenic strain UT5600.

Probing the surface localization of Bla. Surface expression of the Bla moiety was further verified by protease accessibility. Because externally added macromolecules cannot penetrate through the outer membrane, extracellular protease treatment of physiologically intact cells has been used to provide evidence for the surface localization of target proteins. Trypsin treatment of intact JK321(pABETU6), JK321(pABETU7), and JK321(pABETU8) led to the disappearance of the Bla-EstA fusion proteins FP6, FP7, and FP8, respectively, as assessed by Western blots (Fig. 3A). In contrast, Bla located in the periplasm was not susceptible to protease treatment. Consistently, whole-cell immunoblot analysis clearly indicates that the Bla moiety of these fusion proteins is exposed on the surface of *E. coli* (Fig. 3B). Thus, the Bla-EstA fusion proteins FP6 through FP8 were expected to contain a complete translocator domain which is necessary for the surface expression of the N-terminally fused passenger domain.

For the quantitative measurement of surface-displayed Bla moieties, *E. coli* cells expressing the fusion proteins were analyzed by fluorescence-activated cell sorting (FACS). The *E. coli* cells were probed with anti-Bla monoclonal antibody and then fluorescently stained with fluorescein isothiocyanate-conjugated anti-mouse IgG to allow FACS analysis. Consistent with the result from protease accessibility, only *E. coli* cells harboring pABETU6, pABETU7, and pABETU8 were fluorescently stained, indicating that Bla moieties were surface localized in an accessible form (Fig. 4). Furthermore, the fluorescence intensity of each sample was proportional to the expression levels of fusion proteins, as shown by whole-cell immunoblots (Fig. 4A). In contrast, *E. coli* cells harboring

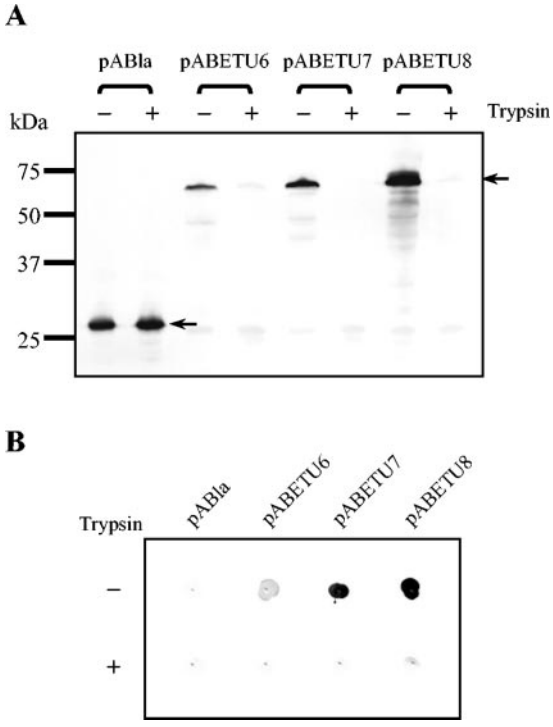

FIG. 3. Protease accessibility of fusion proteins assessed by (A) Western blots and (B) whole-cell immunoblots. Samples were prepared and analyzed as described in the legend of Fig. 2. Tryptic digestion of physiologically intact cells was performed as described in Materials and Methods.

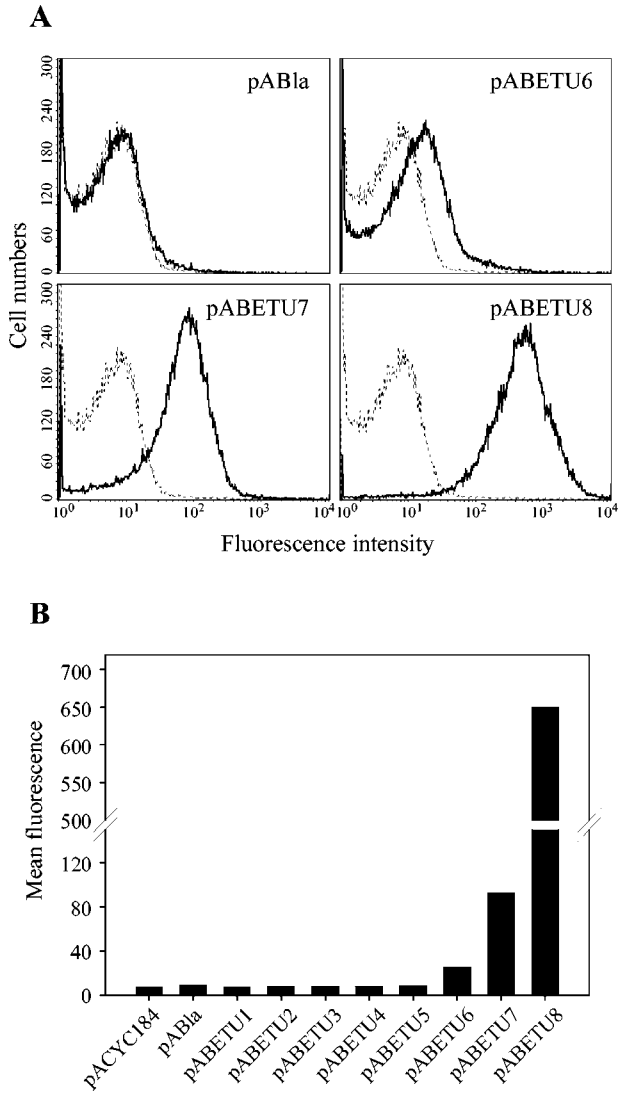

FIG. 4. (A) FACS histograms of recombinant *E. coli* cells to determine surface localization of Bla. The *E. coli* cell line harboring pACYC184 (vector) was used as the negative control, and the corresponding histogram (dotted line) was superimposed on results (solid line) with *E. coli* expressing periplamsic Bla (pABla) or Bla-EstA fusion proteins (indicated recombinant plasmid). (B) Mean fluorescence intensities of *E. coli* cells expressing periplasmic Bla and Bla-EstA fusion proteins.

pABETU1 to pABETU5 and the control construct (pABla) were not fluorescently stained (Fig. 4B). The surface expression of the Bla moiety of the fusion proteins having domains longer than the EstA β8 domain were also examined. Although the expression levels of fusion proteins were similar, the EstA β8 domain exported the maximal amount of Bla moieties to the cell surface (data not shown). Taken together, these observations demonstrate that (i) the EstA β8 domain provides the sufficient structure necessary for the transport of an N-terminal passenger domain to the cell surface and (ii) the region between L297 in the EstA β8 domain and E317 in the EstA β6 domain could contribute to the passenger domain translocation.

Growth kinetics and viability of recombinant *E. coli* cells. Generally, overproduction of the outer membrane-linked proteins often results in changes of the outer membrane structure and consequently in periplasmic enzyme leakages and cell death (9, 14). In order to investigate whether surface expression of the Bla-EstA fusion proteins inhibits the growth of host cells, growth kinetics of *E. coli* cells expressing periplasmic Bla (pABla) or the Bla-EstA fusion protein FP8 (pABETU8) were compared. As shown in Fig. 5, the growth rates were similar for all *E. coli* transformants, irrespective of the presence of the Bla-EstA fusion proteins. Furthermore, we examined host cell viability and outer membrane integrity of the Bla-EstA fusion proteins expressing *E. coli* cells and the control cells, as estimated by axonal dye $DiBAC_4(3)$, whose accumulation within bacterial cells is favored by a reduction in the magnitude of the membrane potential (11). The constitutive expression of the Bla-EstA fusion proteins had no influence on cell viability even at late stationary phase (Fig. 5). From these observations, we concluded that the EstA translocator domain-mediated surface expression does not appear to influence host cell growth, viability, or the integrity of the outer membrane.

Assessment of enzymatic activity of surface-exposed Bla. All JK321 transformants expressing fusion proteins FP1 through FP8 as well as the periplasmic Bla were able to grow normally both on solid and in liquid LB medium containing ampicillin (100 μg/ml). Furthermore, FP8-expressing *E. coli* cells were able to grow in the presence of 200 μg of ampicillin/ml, although the growth of the cells was slightly retarded. This result suggests that all Bla-EstA fusion proteins and the periplasmic Bla are enzymatically active. Since the poorly expressed fusion proteins FP1 through FP5 may not form a correct folding structure in the outer membrane, the ampicillin resistance in transformants expressing these fusion proteins might be conferred by an unfolded or a partially folded polypeptide in the periplasm.

In order to find out whether the surface-exposed Bla shows enzymatic activity, penicillin G was employed as the substrate since it does not readily diffuse through the outer membrane (38) and thus has been frequently used for determination of surface-displayed Bla activity (12, 29). As shown in Fig. 6, the Bla-EstA fusion protein FP8-expressing *E. coli* cells showed

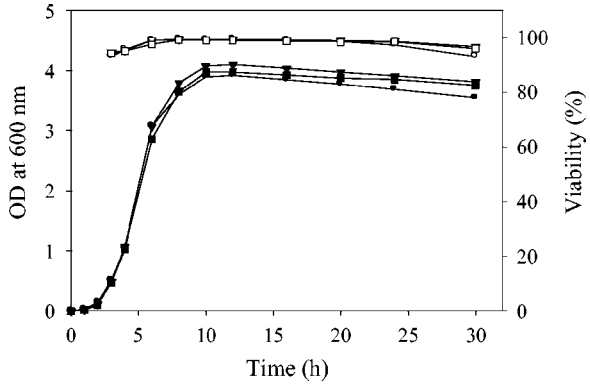

FIG. 5. Growth kinetics and viability of *E. coli* cells expressing the Bla-EstA fusion proteins and periplasmic Bla. The *E. coli* cells harboring pACYC184 (vector) (●), pABla (▼), and pABETU8 (■) were grown in LB broth, and the viability of each recombinant *E. coli* cell suspension (open symbols) was estimated by using $DiBAC_4(3)$ staining (determined in duplicate without significant variation).

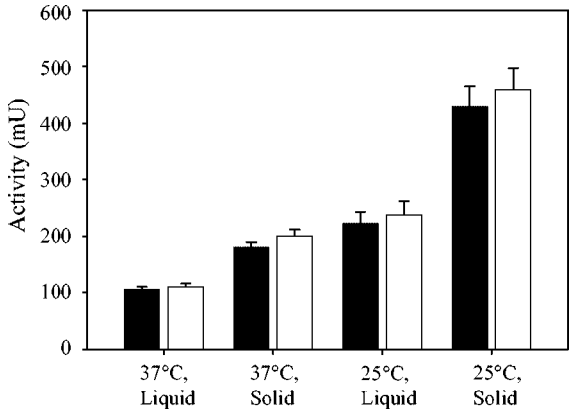

FIG. 6. Whole-cell Bla activity of *E. coli* cells expressing the Bla-EstA fusion proteins. The *E. coli* cell line harboring pABETU8 was grown on an LB agar plate (solid) or in LB broth (liquid) at indicated temperatures with (open bars) and without (filled bars) ampicillin. Whole-cell Bla activities are shown as the mean values, representing the results of five independent experiments, which are calculated for the amounts of bacteria present in 1 ml of a suspension with an OD_{575} of 1.0 ($\sim 2.5 \times 10^9$ CFU). One unit of Bla activity is defined as the amount of enzyme that hydrolyzes 1 μmol of penicillin G per min.

whole-cell Bla activity, and this whole-cell activity was significantly influenced by cultivation conditions. In contrast, *E. coli* cells expressing periplasmic Bla (pABla) have only negligible levels of Bla activity in this experimental condition (data not shown). Lowering the growth temperature of FP8-expressing *E. coli* cells resulted in a significant increase of whole-cell Bla activity as shown previously by others (12, 29). Interestingly, FP8-expressing *E. coli* cells grown on solid LB medium showed much higher Bla activity than the cells grown in liquid LB medium. Consistently, the cells grown on solid LB medium showed the higher mean fluorescence intensity, indicating that more Bla moieties were displayed on the cell surface, as determined by FACS analysis (data not shown). Also, when FP8-expressing *E. coli* cells were grown in the presence of ampicillin, the whole-cell Bla activity was found to increase.

DISCUSSION

In this report, we described the N-terminal fusion display of the normally periplasmic enzyme Bla on the surface of *E. coli* using the EstA translocator domain. The enzymatically active Bla moiety of the Bla-EstA fusion proteins was efficiently exposed on the surface of *E. coli* without compromising cell viability, as evidenced by whole-cell immunoblots, protease accessibility, flow cytometry analysis, and whole-cell Bla activity.

From the data shown, we demonstrated that the translocator domain both necessary and sufficient for surface expression could be limited to the amino acids encompassing L297 through to F622 in EstA and that the expression levels of each fusion protein were significantly dependent on the length of the predicted linking region. Although EstA β6 and EstA β7 domains were capable of translocating the passenger protein through the outer membrane, their targeting to the outer membrane was partly impaired and/or needed extended time for stable β-barrel structure compared with the EstA β8 domain. We therefore assume that a region between L297 and E317 could somehow contribute to β-barrel function, such as facilitating the interaction with the outer membrane and/or enhancing the stability of the β-barrel structure in the membrane. These results, taken together with the secondary structure prediction, led us to propose a possible topological model, depicted in Fig. 7. In this model, 12 β-strands, which consist of 11 amphipathic β-strands and one more hypothetical β-strand, together with an α-helical structure are supposed to form a β-barrel. A recent investigation of the autotransporter NalP from *Neisseria meningitidis* revealed that a single translocator domain, which is composed of a 12-stranded β-barrel and an N-terminal α-helix, is sufficient for the transport of the N-terminal passenger domain (40). An additional stretch of amino acids from L297 to E317 together with an α-helical structure are assumed to serve as a linking region for efficient surface expression and for stable membrane structure. It has been shown that many autotransporter proteins, such as the IgA protease of *Neisseria* (24), the VirG protein of *Shigella* (46), the AIDA-I protein of *E. coli* (36), and the Hia adhesion of *Haemophilus influenzae* (45), require a linking region for their proper folding in the outer membrane and the translocation of passenger protein on the surface.

In all applications that use surface display technology, viability of host cells is a critical issue. For example, for high-throughput screening of enzyme or polypeptide libraries, the maintenance of initial library diversity depends mostly on the viability of host cells expressing target proteins or polypeptides (8, 9). As assessed by FACS analysis, the fluorescence intensity of the Bla-EstA fusion protein FP8-expressing *E. coli* cells was prominent compared with other surface display systems such as *Pseudomonas syringae* ice nucleation protein-based bacterial display (20, 21), indicating that the cells displayed larger amounts of heterologous moieties in an accessible form at the surface. However, the presence of the EstA-Bla fusion proteins in the outer membrane appears to have no influence on growth rate or cell viability. Due to the characteristic feature of oxonol dye, a membrane potential-dependent probe, the host cell viability assay also implies that the outer membrane integrity is intact. In addition, we examined the possibility of FACS selection of *E. coli* cells expressing the EstA-Bla fusion proteins from the mixture with the control cells, and thus, viable cells expressing surface-exposed Bla could be successfully isolated without the need for PCR and subcloning (data not shown).

Besides host cell viability, the biological activity of the surface-exposed heterologous passengers should also be considered. The enzymatic activity of the surface-exposed Bla was shown by whole-cell penicillin G hydrolysis, and this whole-cell activity significantly varied with cultivation conditions including the growth temperature, the type of medium, and the presence of substrate, ampicillin. However, the surface-expressed fusion proteins FP6 through FP8 seem to have the Bla activity in the periplasmic space because the surface-exposed Bla by itself does not seem to completely degrade ampicillin molecules present in the liquid medium before they reach the periplasm by diffusion. This Bla activity probably arises from the translocation intermediates whose C-terminal β-domain is inserted in the outer membrane, and the N-terminal Bla passengers exist in the periplasmic side with the partially folded state. Previous reports demonstrated that the folding of the passenger domain takes place in the periplasm before, or at

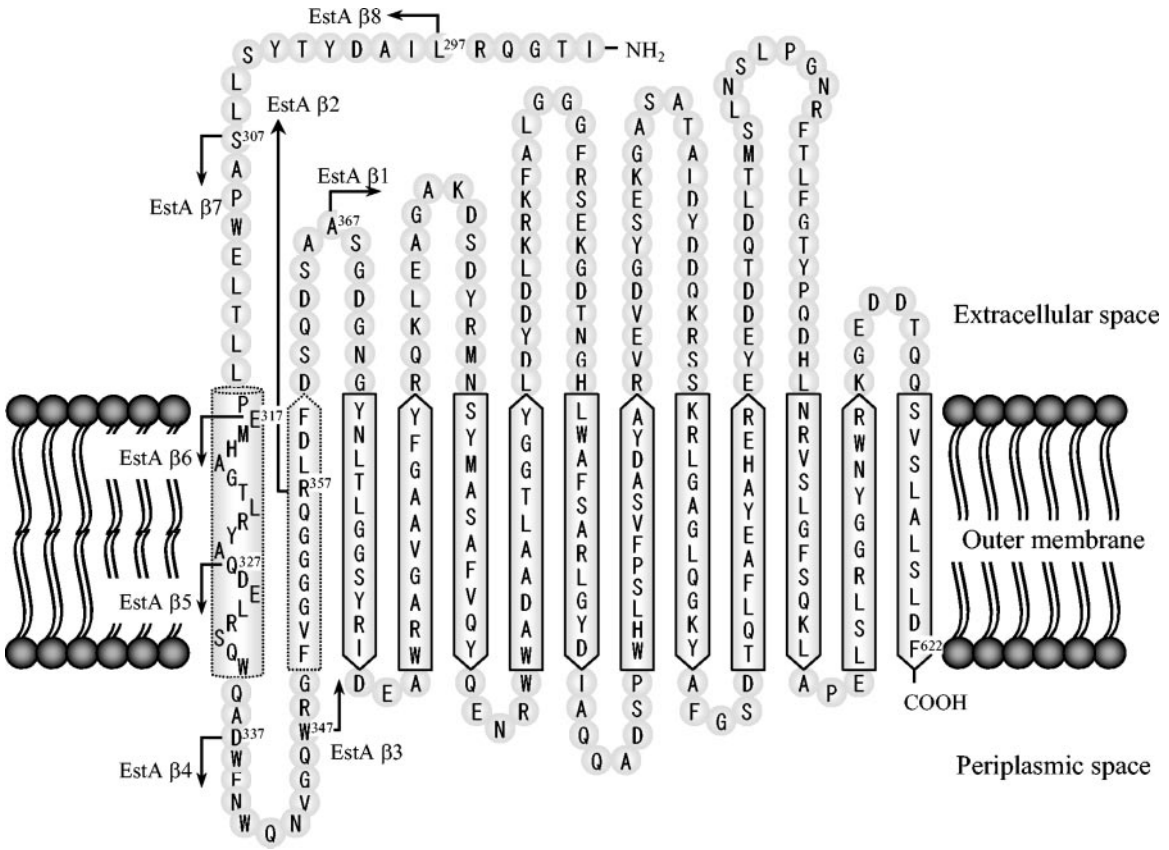

FIG. 7. Possible topological model of the organization of the EstA β-domain in the outer membrane. The C-terminal β-domain of EstA might be composed of 12 amphipathic β-strands (pentagons) and one α-helical structure (cylinder). Eleven amphipathic β-strands (solid lines) are clearly predicted by the 3D-PSSM program within the C-terminal region Y374 to F622 as shown by Wilhelm et al. (49), while one more β-strand and an α-helix are hypothetical (dotted line). The first amino acid residues of the N-terminally truncated EstA β-domains are indicated by arrows.

least simultaneously with, translocation through the outer membrane (6, 39). Alternatively, the residual Bla activity in the periplasm, resulting from proteolytic degradation of fusion proteins, might protect the penicillin binding proteins from inactivation by ampicillin.

A successful surface display system should satisfy several requirements. First, it should be compatible with the foreign moiety and consequently guarantee the biological activity of surface-exposed passenger protein. Second, a maximum number of fully exposed foreign moieties per cell should be presented. Third, the expression of the surface-exposed passenger moiety should occur without compromising cell viability or the outer membrane integrity. From our data described here, the EstA translocator domain-based surface display of heterologous passenger protein mostly satisfies these requirements. Since *P. putida* is a well-known solvent-tolerant strain and has been used in environmental biotechnology (44) as well as in biotechnological production processes in two-phase systems as a whole-cell biocatalyst (31), we are trying to employ this EstA translocator domain-mediated surface display system for the development of whole-cell biocatalysts using *P. putida* as a host strain.

ACKNOWLEDGMENT

We thank T. F. Meyer for providing us with *E. coli* strain JK321.

REFERENCES

1. **Agterberg, M., H. Adriaanse, A. van Bruggen, M. Karperien, and J. Tommassen.** 1990. Outer-membrane PhoE protein of *Escherichia coli* K-12 as an exposure vector: possibilities and limitations. Gene **88:**37–45.
2. **Altschul, S. F., T. L. Madden, A. A. Schaffer, J. Zhang, Z. Zhang, W. Miller, and D. J. Lipman.** 1997. Gapped BLAST and PSI-BLAST: a new generation of protein database search programs. Nucleic Acids Res. **25:**3389–3402.
3. **Benhar, I.** 2001. Biotechnological applications of phage and cell display. Biotechnol. Adv. **19:**1–33.
4. **Bingle, W. H., J. F. Nomellini, and J. Smit.** 1997. Cell-surface display of a *Pseudomonas aeruginosa* strain K pilin peptide within the paracrystalline S-layer of *Caulobacter crescentus*. Mol. Microbiol. **26:**277–288.
5. **Bolivar, F.** 1978. Construction and characterization of new cloning vehicles. III. Derivatives of plasmid pBR322 carrying unique EcoRI sites for selection of EcoRI generated recombinant DNA molecules. Gene **4:**121–136.
6. **Brandon, L. D., and M. B. Goldberg.** 2001. Periplasmic transit and disulfide bond formation of the autotransported *Shigella* protein IcsA. J. Bacteriol. **183:**951–958.
7. **Chang, H. J., S. Y. Sheu, and S. J. Lo.** 1999. Expression of foreign antigens on the surface of *Escherichia coli* by fusion to the outer membrane protein TraT. J. Biomed. Sci. **6:**64–70.
8. **Chen, W., and G. Georgiou.** 2002. Cell-surface display of heterologous proteins: from high-throughput screening to environmental applications. Biotechnol. Bioeng. **79:**496–503.
9. **Daugherty, P. S., M. J. Olsen, B. L. Iverson, and G. Georgiou.** 1999. Development of an optimized expression system for the screening of antibody libraries displayed on the *Escherichia coli* surface. Protein Eng. **12:**613–621.
10. **Desvaux, M., N. J. Parham, and I. R. Henderson.** 2004. The autotransporter secretion system. Res. Microbiol. **155:**53–60.
11. **Epps, D. E., M. L. Wolfe, and V. Groppi.** 1994. Characterization of the steady-state and dynamic fluorescence properties of the potential-sensitive dye bis-(1,3-dibutylbarbituric acid)trimethine oxonol (diBA-$C_4(3)^-$) in model systems and cells. Chem. Phys. Lipids **69:**137–150.
12. **Francisco, J. A., C. F. Earhart, and G. Georgiou.** 1992. Transport and

anchoring of β-lactamase to the external surface of *Escherichia coli*. Proc. Natl. Acad. Sci. USA **89:**2713–2717.
13. **Fuchs, P., F. Breitling, S. Dubel, T. Seehaus, and M. Little.** 1991. Targeting recombinant antibodies to the surface of *Escherichia coli*: fusion to a peptidoglycan associated lipoprotein. Bio/Technology **9:**1369–1372.
14. **Georgiou, G., C. Stathopoulos, P. S. Daugherty, A. R. Nayak, B. L. Iverson, and R. Curtiss III.** 1997. Display of heterologous proteins on the surface of microorganisms: from the screening of combinatorial libraries to live recombinant vaccines. Nat. Biotechnol. **15:**29–34.
15. **Henderson, I. R., and J. P. Nataro.** 2001. Virulence functions of autotransporter proteins. Infect. Immun. **69:**1231–1243.
16. **Henderson, I. R., F. Navarro-Garcia, and J. P. Nataro.** 1998. The great escape: structure and function of the autotransporter proteins. Trends Microbiol. **6:**370–378.
17. **Jepras, R. I., J. Carter, S. C. Pearson, F. E. Paul, and M. J. Wilkinson.** 1995. Development of a robust flow cytometric assay for determining numbers of viable bacteria. Appl. Environ. Microbiol. **61:**2696–2701.
18. **Jose, J., R. Bernhardt, and F. Hannemann.** 2002. Cellular surface display of dimeric Adx and whole cell P450-mediated steroid synthesis on *E. coli*. J. Biotechnol. **95:**257–268.
19. **Jose, J., J. Kramer, T. Klauser, J. Pohlner, and T. F. Meyer.** 1996. Absence of periplasmic DsbA oxidoreductase facilitates export of cysteine-containing passenger proteins to the *Escherichia coli* cell surface via the Iga_{β} autotransporter pathway. Gene **178:**107–110.
20. **Jung, H. C., S. Ko, S. J. Ju, E. J. Kim, M. K. Kim, and J. G. Pan.** 2003. Bacterial cell surface display of lipase and its randomly mutated library facilitates high-throughput screening of mutants showing higher specific activities. J. Mol. Catal. B Enzym. **26:**177–184.
21. **Jung, H. C., J. M. Lebeault, and J. G. Pan.** 1998. Surface display of *Zymomonas mobilis* levansucrase by using the ice-nucleation protein of *Pseudomonas syringae*. Nat. Biotechnol. **16:**576–580.
22. **Kelley, L. A., R. M. MacCallum, and M. J. Sternberg.** 2000. Enhanced genome annotation using structural profiles in the program 3D-PSSM. J. Mol. Biol. **299:**499–520.
23. **Kjaergaard, K., H. Hasman, M. A. Schembri, and P. Klemm.** 2002. Antigen 43-mediated autotransporter display, a versatile bacterial cell surface presentation system. J. Bacteriol. **184:**4197–4204.
24. **Klauser, T., J. Krämer, K. Otzelberger, J. Pohlner, and T. F. Meyer.** 1993. Characterization of the *Neisseria* Iga_{β}-core. The essential unit for outer membrane targeting and extracellular protein secretion. J. Mol. Biol. **234:**579–593.
25. **Klemm, P., and M. A. Schembri.** 2000. Fimbriae-assisted bacterial surface display of heterologous peptides. Int. J. Med. Microbiol. **290:**215–221.
26. **Konieczny, M. P., M. Suhr, A. Noll, I. B. Autenrieth, and M. A. Schmidt.** 2000. Cell surface presentation of recombinant (poly-) peptides including functional T-cell epitopes by the AIDA autotransporter system. FEMS Immunol. Med. Microbiol. **27:**321–332.
27. **Kornacker, M. G., and A. P. Pugsley.** 1990. The normally periplasmic enzyme β-lactamase is specifically and efficiently translocated through the *Escherichia coli* outer membrane when it is fused to the cell-surface enzyme pullulanase. Mol. Microbiol. **4:**1101–1109.
28. **Kramer, U., K. Rizos, H. Apfel, I. B. Autenrieth, and C. T. Lattemann.** 2003. Autodisplay: development of an efficacious system for surface display of antigenic determinants in *Salmonella* vaccine strains. Infect. Immun. **71:**1944–1952.
29. **Lattemann, C. T., J. Maurer, E. Gerland, and T. F. Meyer.** 2000. Autodisplay: functional display of active β-lactamase on the surface of *Escherichia coli* by the AIDA-I autotransporter. J. Bacteriol. **182:**3726–3733.
30. **Lee, S. Y., J. H. Choi, and Z. Xu.** 2003. Microbial cell-surface display. Trends Biotechnol. **21:**45–52.
31. **Lee, S. Y., and J. S. Rhee.** 1994. Hydrolysis of triglyceride by the whole cell of *Pseudomonas putida* 3SK in two-phase batch and continuous reactors systems. Biotechnol. Bioeng. **44:**437–443.
32. **Lee, S. Y., and J. S. Rhee.** 1993. Production and partial purification of a lipase from *Pseudomonas putida* 3SK. Enzyme Microb. Technol. **15:**617–623.
33. **Lu, Z., K. S. Murray, V. Van Cleave, E. R. LaVallie, M. L. Stahl, and J. M. McCoy.** 1995. Expression of thioredoxin random peptide libraries on the *Escherichia coli* cell surface as functional fusions to flagellin: a system designed for exploring protein-protein interactions. Bio/Technology **13:**366–372.
34. **Marchler-Bauer, A., J. B. Anderson, C. DeWeese-Scott, N. D. Fedorova, L. Y. Geer, S. He, D. I. Hurwitz, J. D. Jackson, A. R. Jacobs, C. J. Lanczycki, C. A. Liebert, C. Liu, T. Madej, G. H. Marchler, R. Mazumder, A. N. Nikolskaya, A. R. Panchenko, B. S. Rao, B. A. Shoemaker, V. Simonyan, J. S. Song, P. A. Thiessen, S. Vasudevan, Y. Wang, R. A. Yamashita, J. J. Yin, and S. H. Bryant.** 2003. CDD: a curated Entrez database of conserved domain alignments. Nucleic Acids Res. **31:**383–387.
35. **Maurer, J., J. Jose, and T. F. Meyer.** 1997. Autodisplay: one-component system for efficient surface display and release of soluble recombinant proteins from *Escherichia coli*. J. Bacteriol. **179:**794–804.
36. **Maurer, J., J. Jose, and T. F. Meyer.** 1999. Characterization of the essential transport function of the AIDA-I autotransporter and evidence supporting structural predictions. J. Bacteriol. **181:**7014–7020.
37. **Mesnage, S., M. Weber-Levy, M. Haustant, M. Mock, and A. Fouet.** 1999. Cell surface-exposed tetanus toxin fragment C produced by recombinant *Bacillus anthracis* protects against tetanus toxin. Infect. Immun. **67:**4847–4850.
38. **Nikaido, H., and S. Normark.** 1987. Sensitivity of *Escherichia coli* to various β-lactams is determined by the interplay of outer membrane permeability and degradation by periplasmic β-lactamases: a quantitative predictive treatment. Mol. Microbiol. **1:**29–36.
39. **Oliver, D. C., G. Huang, E. Nodel, S. Pleasance, and R. C. Fernandez.** 2003. A conserved region within the *Bordetella pertussis* autotransporter BrkA is necessary for folding of its passenger domain. Mol. Microbiol. **47:**1367–1383.
40. **Oomen, C. J., P. Van Ulsen, P. Van Gelder, M. Feijen, J. Tommassen, and P. Gros.** 2004. Structure of the translocator domain of a bacterial autotransporter. EMBO J. **23:**1257–1266.
41. **Rizos, K., C. T. Lattemann, D. Bumann, T. F. Meyer, and T. Aebischer.** 2003. Autodisplay: efficacious surface exposure of antigenic UreA fragments from *Helicobacter pylori* in *Salmonella* vaccine strains. Infect. Immun. **71:**6320–6328.
42. **Rose, R. E.** 1988. The nucleotide sequence of pACYC184. Nucleic Acids Res. **16:**355.
43. **Samuelson, P., M. Hansson, N. Ahlborg, C. Andreoni, F. Gotz, T. Bachi, T. N. Nguyen, H. Binz, M. Uhlen, and S. Stahl.** 1995. Cell surface display of recombinant proteins on *Staphylococcus carnosus*. J. Bacteriol. **177:**1470–1476.
44. **Shimazu, M., A. Nguyen, A. Mulchandani, and W. Chen.** 2003. Cell surface display of organophosphorus hydrolase in *Pseudomonas putida* using an ice-nucleation protein anchor. Biotechnol. Prog. **19:**1612–1614.
45. **St. Geme, J. W., III, and D. Cutter.** 2000. The *Haemophilus influenzae* Hia adhesin is an autotransporter protein that remains uncleaved at the C terminus and fully cell associated. J. Bacteriol. **182:**6005–6013.
46. **Suzuki, T., M. C. Lett, and C. Sasakawa.** 1995. Extracellular transport of VirG protein in *Shigella*. J. Biol. Chem. **270:**30874–30880.
47. **Upton, C., and J. T. Buckley.** 1995. A new family of lipolytic enzymes? Trends Biochem. Sci. **20:**178–179.
48. **Valls, M., S. Atrian, V. de Lorenzo, and L. A. Fernandez.** 2000. Engineering a mouse metallothionein on the cell surface of *Ralstonia eutropha* CH34 for immobilization of heavy metals in soil. Nat. Biotechnol. **18:**661–665.
49. **Wilhelm, S., J. Tommassen, and K. E. Jaeger.** 1999. A novel lipolytic enzyme located in the outer membrane of *Pseudomonas aeruginosa*. J. Bacteriol. **181:**6977–6986.
50. **Xu, Z., and S. Y. Lee.** 1999. Display of polyhistidine peptides on the *Escherichia coli* cell surface by using outer membrane protein C as an anchoring motif. Appl. Environ. Microbiol. **65:**5142–5147.